Nonlinear absorption of intense short pulse laser over a metal surface embedded with nanoparticles

ASHOK KUMAR AND A.L. VERMA
Department of Physics, Amity Institute of Applied Sciences, ASET, Amity University, Noida, India

(RECEIVED 15 January 2011; ACCEPTED 2 June 2011)

Abstract

The anomalous absorption of laser, incident at an arbitrary angle of incidence on a metal surface embedded with nanoparticles, is studied. The electrons inside a nanoparticle resonantly absorb laser energy when the laser frequency equals the frequency of surface charge oscillations of the nanoparticle. A monolayer of nanoparticles of radius $r_{np0} \approx$ 50 A with inter-particle separation $d \sim 10 r_{np0}$ can cause up to 40% reduction of the reflection of p-polarized laser light. The absorption coefficient increases with the angle of incidence and has a sharp peak at a resonant frequency width of about 1%. At high laser power, even if the nanoparticles are initially off resonant with the laser, the particle heating and subsequent expansion reduces the resonance frequency, and the resonance absorption is realized after a time delay. The delay is found to be directly proportional to the cluster size and inversely proportional to the laser intensities.

Keywords: Anaomalous absorption; intense short pulse laser; nanoparticles

1. INTRODUCTION

Enhancement in laser absorption over metal surfaces is an important issue in many practical applications e.g., pulsed laser deposition of films and laser ablation of materials (Stratakis *et al.*, 2009; Chen & Mao, 2008; Taylor & Helvajian, 2009; Shukla & Khare, 2010; Bagchi *et al.*, 2008). It has been shown that the presence of nano- and micro-structures over a metal surface can cause very significant reduction in laser reflectivity (Vorobyev & Guo, 2005a, 2005b, 2006, 2008; Vorobyev *et al.*, 2009; Kaakkunen *et al.*, 2009). The synthesis and study of nanoparticles and nanostructured surfaces of various elements are of great interest both in technological applications and for fundamental research (Kreibig & Vollmer, 1995; Maier, 2007; Dhareshwar & Chaurasia, 2008; Eliezer *et al.*, 2004, 2005; Fazio *et al.*, 2009; Gamaly *et al.*, 2000; Nolte *et al.*, 1999; Menendez-Manjon *et al.*, 2010; Thareja & Sharma, 2006; Wieger *et al.*, 2006; Wolowsky *et al.*, 2007; Zavestovskaya, 2010).

During the interaction between a laser pulse and a metal, the laser energy is absorbed in the electronic system of the metal resulting in the generation of highly excited non-thermalized electrons (Fujimoto *et al.*, 1984; Elsayed-Ali

et al., 1987; Jasiak *et al.*, 2010; Bigot *et al.*, 2000). The electronic system subsequently relaxes by both, e–e interaction to a hot Fermi distribution as well as by energy transfer to the lattice *via* e–ph collisions. The laser interacting with a metal surface delivers its energy directly to conduction electrons, which gets thermalized almost instantaneously, elevating the electron temperature. Hwang *et al.* (2009) attributed the reflectivity reduction to increase in effective surface area of the metal surface due to the presence of nanoparticles. This may be true when the laser frequency is away from the surface plasmon resonance. Ahmad and Tripathi (2006) have studied the absorption of laser normally incident on a metal surface embedded with nanoparticles. When the laser frequency equals the natural frequency of surface plasmon oscillations, there is very significant absorption of surface plasma waves (Kumar & Tripathi, 2007). Akhmanov *et al.* (1985) have given an elegant review of physical effects taking place at the surface of the metals by high-power radiation. Rajeev *et al.* (2003) have demonstrated a method to enhance hard X-ray bremsstrahlung by coating nanoparticles on optically smooth metal targets. Pustovalov (2005) studied the heating of spherical solid metal particle by laser pulse.

In this paper, we study linear and nonlinear absorption over a metal surface in the presence of metallic nanoparticles at oblique incidence. The total field inside the nanoparticle will be strongly absorbed when the laser frequency resonates

---

Address correspondence and reprint requests to: Ashok Kumar, Department of Physics, Amity Institute of Applied Sciences, ASET, Amity University, Noida, U.P., 201303, India. E-mail: ashokkumarthakur@yahoo.com

with the surface charge oscillations. The combined fields of incident and reflected radiation impart quiver velocity to electrons inside the nanoparticles. The quiver velocity is resonantly large when the laser frequency equals the surface plasma frequency of the nanoparticles. It also has a component in phase with the laser field and gives rise to power absorption from the laser. At high power, the laser causes an increase in electron temperature, and a subsequent expansion of the nanoparticles leading to a reduction in plasmon frequency. Even if initially the laser frequency is below the surface plasmon frequency but the laser power is high, the surface plasmon resonance can be realized after a time delay.

In Section 2, we study the linear absorption of laser light over a smooth metal surface having nonexpanding nanoparticles and in Section 3, we study the nonlinear power absorbed inside expanding nanoparticles. The discussion of the obtained result is given in Section 4.

2. LINEAR ABSORPTION OF LASER INSIDE NONEXPANDING NANOPARTICLES

Consider a metal-free space interface ($z = 0$) with $z > 0$ metal and $z < 0$ free space. A layer of metallic nanoparticles is spread on the metal surface with interparticle separation d (Fig. 1). A p-polarized laser is incident on the interface at angle of incidence θ,

$$\mathbf{E}_i = \mathbf{A}_0 e^{-(\omega t - \mathbf{k}_1 \cdot \mathbf{r})}, \tag{1}$$

where $\mathbf{k}_1 = k_{1z}\, \mathbf{z} + k_{1x}\, \mathbf{x}$, $k_{1z} = (\omega/c) \cos\theta$, $k_{1x} = (\omega/c)\eta \sin\theta$, $A_{0z} = (-\,k_{1x}/k_{1z})\, A_{0x}$ and effective refractive index of the metal is $\eta = \sqrt{\varepsilon_{\text{eff}}}$, ε_{eff} being effective dielectric constant.

The reflected laser from the metal surface is

$$\mathbf{E}_r = \mathbf{A}_r e^{-(\omega t - \mathbf{k}_1' \cdot \mathbf{r})}, \quad A_{rz} = (-k_{1x}/k_{1z})A_{rx}, \tag{2}$$

where $\vec{k}_1' = -k_{1z}\hat{z} + k_{1x}\hat{x}$.

The transmitted field inside the metal is

$$\mathbf{E}_t = \mathbf{A}_t\, e^{-(\omega t - \vec{k}_2 \cdot \vec{r})} A_{tz} = (-k_{2x}/k_{2z})A_{tx}, \tag{3}$$

where $\vec{k}_2 = k_{1x}\hat{x} + k_{2z}\hat{z}$, $k_{2z} = (\omega^2 \varepsilon_2/c^2 - k_{1x}^2)^{1/2}$, $\varepsilon_2 = \varepsilon_L - \omega_p^2/\omega^2$, ε_L is the lattice permittivity, and ω_P^2 is the metal plasma frequency defined as $\omega_P^2 \equiv (4\pi n_0 e^2/m)^{1/2}$, $-e$ and m are the electronic charge and mass, respectively, n_0 is the electron density of the metal surface. If one ignores the presence of nanoparticles, one may employ the condition of continuity E_x and $(\varepsilon\, E_z)$ at $z = 0$ to obtain

$$A_{tx} = 2 A_{0x} \Big/ \left(1 + \eta^2 \frac{k_{1z}}{k_{2z}}\right), \tag{4}$$

$$A_{rx} = A_{0x}\left(1 - \eta^2 \frac{k_{1z}}{k_{2z}}\right) \Big/ \left(1 + \eta^2 \frac{k_{1z}}{k_{2z}}\right). \tag{5}$$
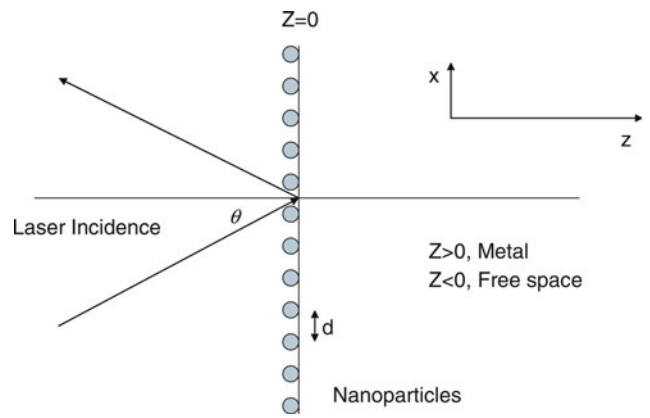

Fig. 1. (Color online) Schematic of obliquely incident laser over a metal surface embedded with metal nanoparticles.

The amplitude reflection coefficient is

$$R = \left(1 - \eta^2 \frac{k_{1z}}{k_{2z}}\right) \Big/ \left(1 + \eta^2 \frac{k_{1z}}{k_{2z}}\right). \tag{6}$$

Upon reflection from a conducting surface, below the plasma edge $\omega < \omega_P/\sqrt{\varepsilon_L}$, k_{2z} is complex. Writing $k_{2z} = i\alpha$, where $\alpha = \omega/c \left[\sin^2\theta_i - \eta^2\right]$, the above equation can be written as

$$R = \left(1 + i\eta^2 \frac{k_{1z}}{\alpha}\right) \Big/ \left(1 - i\eta^2 \frac{k_{1z}}{\alpha}\right). \tag{7}$$

The net electric field inside a nanoparticle is

$$\mathbf{E} = (\mathbf{E}_i + \mathbf{E}_r)|_{z=0}. \tag{8}$$

Under the influence of this field, electrons of the nanoparticles execute oscillations with displacement $\vec{\Delta}$

$$\frac{\partial^2 \vec{\Delta}}{\partial t^2} + \frac{\omega_{np}^2}{\beta} \vec{\Delta} = \frac{-e\vec{E}}{m} - \nu \frac{\partial \vec{\Delta}}{\partial t}, \tag{9}$$

where $\omega_{np}^2 = (4\pi n_{np} e^2/m)^{1/2}$, n_{np} is the electron density inside the nanoparticles, ν is the electron-ion collision frequency, β is a parameter depending on the shape of the particle. For a spherical nanoparticle $\beta = 3$.

Taking $\partial/\partial t = -i\omega$, Eq. (8) gives the excursion $\vec{\Delta}$ and electron velocity $\vec{V} = \partial \vec{\Delta}/\partial t$,

$$\vec{\Delta} = \frac{(eA)/m}{\left[\left(\omega^2 - \dfrac{\omega_{np}^2}{\beta}\right) + i\nu\omega\right]} e^{-i\omega t} \quad \text{and} \tag{10}$$

$$\vec{V} = \frac{d\vec{\Delta}}{dt} = \frac{(-i\omega)(eA)/m}{\left[\left(\omega^2 - \dfrac{\omega_{np}^2}{\beta}\right) + i\nu\omega\right]} e^{-i\omega t}. \tag{11}$$

The part of $\vec{V}$ in phase with the electric field gives rise to time average power absorption per electron

$$p_{abs} = \frac{1}{2}\text{Re}\left[-e\vec{E}^{*} \cdot \vec{V}\right] = \frac{e^2 A^2 \nu \omega^2}{2m\left[\left(\omega^2 - \frac{\omega_{np}^2}{\beta}\right)^2 + (\nu^2\omega^2)\right]}, \quad (12)$$

where $*$ denotes the complex conjugate. For inter-nanoparticle separation of d, the number of nanoparticles per unit area is $N = 1/d^2$. Hence, the power absorbed per unit area per unit time by the electrons inside the nanoparticles of radius r_{np} is

$$P_{abs} = \frac{N\left(\frac{4\pi r_{np}^3 n_{np}}{3}\right)e^2 A^2 \nu \omega^2}{2m\left[\left(\omega^2 - \frac{\omega_{np}^2}{\beta}\right)^2 + (\nu^2\omega^2)\right]}$$

$$= \frac{N(\omega_{np}^2 r_{np}^3)A^2 \nu \omega^2}{6\left[\left(\omega^2 - \frac{\omega_{np}^2}{3}\right)^2 + (\nu^2\omega^2)\right]}. \quad (13)$$

If the total incident laser power is P_{in}, then from Eq. (8), the resultant laser field inside is

$$A^2 = 32\pi P_{in}/c\left|1 - i\eta^2 \frac{k_{1z}}{\beta}\right|^2. \quad (14)$$

The fraction of power absorbed or absorption coefficient is

$$F \equiv \frac{P_{abs}}{P_{in}} = \frac{16\pi(\omega_{np}^2 r_{np})(r_{np}^2/d^2)\nu\omega^2}{3c\left[\left(\omega^2 - \frac{\omega_{np}^2}{\beta}\right)^2 + (\nu^2\omega^2)\right]\left|1 - i\eta^2 \frac{k_{1z}}{\alpha}\right|^2}. \quad (15)$$

When the applied frequency is close to the resonant plasmon frequency of the nanoparticle, the absorption is resonantly enhanced leading to very strong absorption of laser energy.

$$F = \frac{16\pi(\omega_{np}^2 r_{np})(r_{np}^2/d^2)}{3c\nu\left|1 - i\eta^2 \frac{k_{1z}}{\alpha}\right|^2} \quad (16)$$

One may note that F increases resonantly as ω approaches $\omega_{np}/\sqrt{\beta}$.

We have solved Eq. (15) numerically for the following typical parameters: $r_{np}/d = 0.03-1$, $r_{np} = 5-15nm$, $\omega_{np} = 4 \times 10^{15}$ rad/sec, $\nu/\omega = 0.01$. In Figure 2, we have plotted the absorption coefficient with laser frequency. The absorption coefficient increases to 0.55 for oblique incidence at 45° compared to 0.30 for normal incidence. Resonance is sharply peaked at laser frequency close to $\omega_{np}/\sqrt{3}$. The absorption coefficient is found to increase on changing the angle of
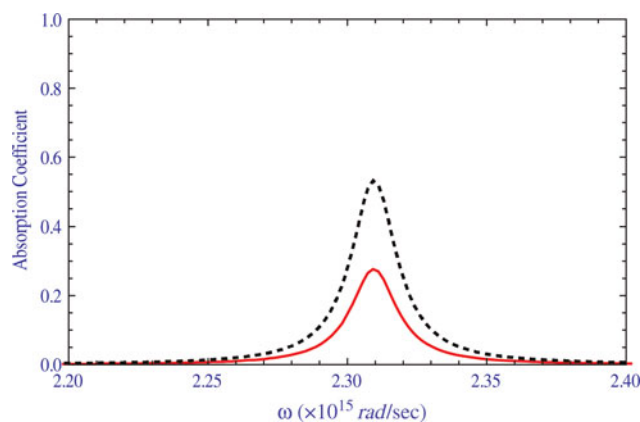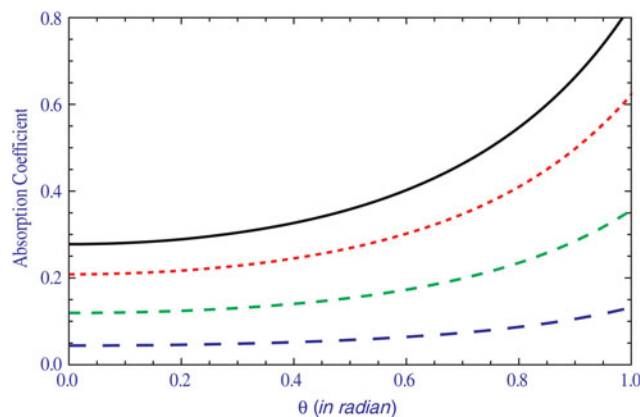

Fig. 2. (Color online) The absorption coefficient is plotted *versus* laser frequency. For typical parameters $r_{np}/d = 0.1$, $r_{np} = 50nm$, $\omega_{np} = 4 \times 10^{15}$ rad/sec, $\nu/\omega = 0.01$, the absorption coefficient increases to 0.55 for oblique incidence at 45° compared to 0.30 for normal incidence. Normal incidence (solid line) and incidence at 45° (dashed line).

incidence at the resonant frequency (Fig. 3). There is a sharp reduction of the absorption coefficient as one moves away from the resonance point. Even a deviation of about 1% away from the resonant frequency reduces the absorption coefficient drastically making the role of resonant absorption inside a nanoparticle insignificant.

3. NONLINEAR ABSORPTION OF LASER INSIDE EXPLODING NANOPARTICLES

Free electrons inside a nanoparticle absorb the laser energy and quickly thermalize to attain a high temperature. Thermal energy is subsequently transferred to the lattice *via* electron-phonon collisions. According to the energy balance

Fig. 3. (Color online) The variation of absorption coefficient as a function of angle of incidence θ is plotted for a fixed laser frequency. The four different frequencies chosen are (i) $\omega = (\omega_{np0}/\sqrt{3})$ (black, solid), (ii) $\omega = (\omega_{np0}/\sqrt{3}) \pm 0.25\%$ (red, small dashed), (iii) $\omega = (\omega_{np0}/\sqrt{3}) \pm 0.5\%$ (green, medium dashed), (iv) $\omega = (\omega_{np0}/\sqrt{3}) \pm 1\%$ (blue, large dashed).
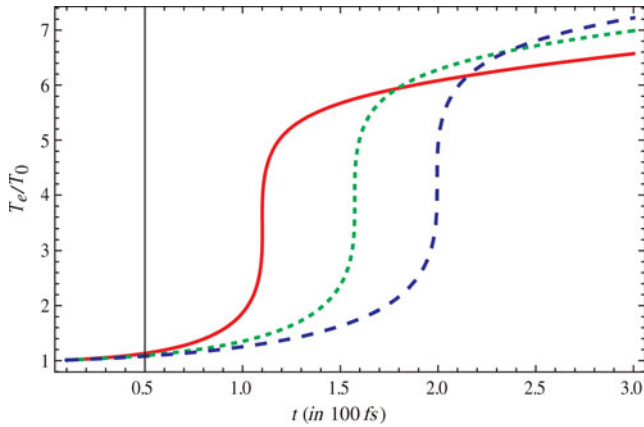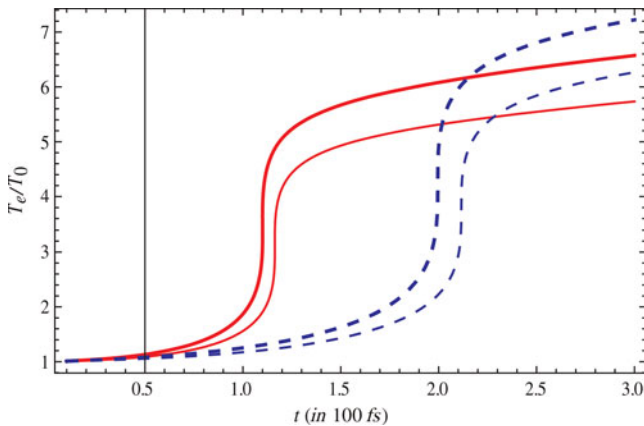
Fig. 4. (Color online) The enhancement in temperature for various cluster size with time (in the unit of 100 fs) for the following parameters. $\omega = 3 \times 10^{15}$ *rad*/sec, $\omega_{np0}/\omega = 4$, $r_{np0}/d = 0.01 - 0.1$, $\nu_0/\omega = 0.01$, $e^2 |E|^2/(3m \omega^2 T_0) = 4$ and the nanoparticle radius (**a**) 2 nm (red, solid), (**b**) 3 nm (green, small dashed), and (**c**) 4 nm (blue, large dashed).

equation, the electron temperature is given by

$$\frac{3}{2}\frac{dT_e}{dt} = \frac{e^2|A|^2\nu\omega^2}{2m\left(\left(\omega^2 - \frac{\omega_{np}^2}{3}\right)^2 + \nu^2\omega^2\right)} - \frac{3}{2}\delta\nu(T_e - T_0), \quad (17)$$

where T_0 is the lattice temperature and the factor characterizing the fractional energy transfer from electrons to ions in each collision $\delta = 2m/m_i$, where m_i is the atomic mass of the metal. For a short intense pulse one can ignore the second term in Eq. (17) representing the energy transfer to the lattice. However the value for δ differ in case of a weakly ionized plasma such as in ionosphere (Gurevich,

Fig. 5. (Color online) The enhancement in temperature with time (in the unit of 100 fs) with the same set of parameters for the nanoparticle radius (**a**) 2 nm (red, solid line), and (**b**) 4 nm (blue, dashed line) for two normalized intensity, $e^2 |E|^2/(3m \omega^2 T_0) = 4$ (thin line) and $e^2 |E|^2/(3m \omega^2 T_0) = 6$ (thick line).
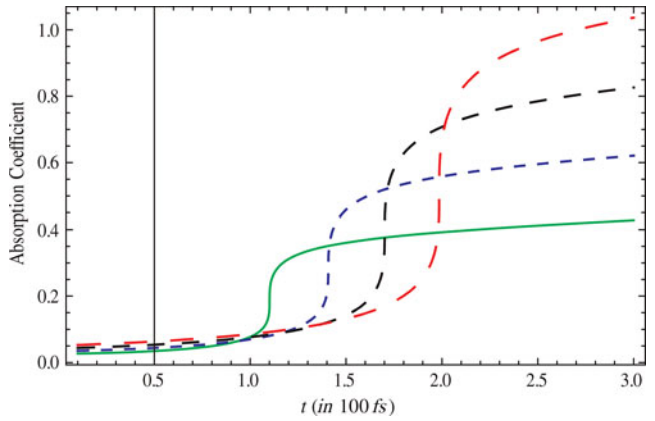
Fig. 6. (Color online) The variation in absorption coefficient with time for different cluster size (**i**) 3 nm (green, solid line), (**ii**) 4 nm (blue, small dashed line), (**iii**) 5 nm (black, medium dashed line), and (**iv**) 6 nm (red, large dashed line).

1978; Meister & Liperovsky, 1996; Kumar & Tripathi, 2007).

The steady-state elevated electron temperature is then

$$\frac{\partial(T_e/T_0)}{\partial t} = \frac{e^2|A|^2\nu}{3m\omega^2 T_0\left(\left(1 - \frac{\omega_{np}^2}{3\omega^2}\right)^2 + \frac{\nu^2}{\omega^2}\right)}. \quad (18)$$

Heated electrons, due to their large partial pressure, leave behind a strong positive charge core, causing ion Coulomb explosion. The core expands at the rate of ion sound speed, $C_s = (T_e/m_i)^{1/2}$, hence the radius of the nanoparticle changes with time as

$$r_{np} = r_{np0} + \int_0^t C_s dt, \quad (19)$$

where r_{np0} is the initial radius of unexpanded nanoparticle.

As the nanoparticle expands, the electron density decreases, keeping the term $\omega_{np}^2 r_{np}^3$ constant. Hence one may express

$$\omega_{np0}^2 r_{np0}^3 = \omega_{np}^2 r_{np}^3, \quad (20)$$

where ω_{np0}^2 refers to the value of plasma frequency inside nanoparticle ω_{np}^2 at radius r_{np0}. The electron-electron collision frequency depends on the electron temperature as

$$\nu = \nu_0(T_e/T_0)^{-3/2}, \quad (21)$$

where ν_0 is the collision frequency at lattice temperature. Eq.

(18) can be simplified as

$$\frac{\partial(T_e/T_0)}{\partial t} = \frac{e^2|E|^2 \nu_0 (T_e/T_0)^{-3/2}}{3m\omega^2 T_0} \left\{ \left[1 - \frac{\omega_{np0}^2}{3\omega^2} \right. \right.$$

$$\times \left. \left(\frac{1}{1 + (C_{s0}(T_e/T_0)^{1/2}/r_{np0})t} \right)^3 \right]^2 \qquad (22)$$

$$\left. + \frac{\nu_0^2 (T_e/T_0)^{-3}}{\omega^2} \right\}^{-1}$$

where $C_{s0} \equiv (T_0/m_i)^{1/2}$.

The absorption coefficient can be obtained as done in Eq. (18),

$$F \equiv \frac{P_{abs}}{P_{in}}$$

$$= \frac{16\pi(\omega_{np0}^2 r_{np0})(r_{np0}^2/d^2)\nu_0 (T_e/T_0)^{-3/2}}{6\,c\omega^2 \left\{ \left[1 - \frac{\omega_{np0}^2}{3\omega^2} \left(\frac{1}{1 + (C_{s0}(T_e/T_0)^{1/2}/r_{np0})t} \right)^3 \right]^2 \right.}. \quad (23)$$

$$\left. + \frac{\nu_0^2 (T_e/T_0)^{-3}}{\omega^2} \right\} \left| 1 - i\eta^2 \frac{k_{1z}}{\alpha} \right|^2$$

We have solved Eqs. (22) and (23) numerically for the following parameters of practical importance: $\omega = 3 \times 10^{15}$ *rad*/sec, $\omega_{np0}/\omega = 3-5$, $r_{np0} = 1-10nm$, $r_{np0}/d = 0.01 - 0.1$, $\nu_0/\omega = 0.01$ and $e^2 |E|^2 / (3m\ \omega^2 T_0) = 4 - 6$.

In Figures 4 and 5, we have plotted T_e / T_0 as a function of time for different values of initial nanoparticle radius and laser intensity. For a given nanoparticle radius the temperature rises sharply at time $t = t_R$. The value of t_R increases with the radius of the nanoparticles as bigger nanoparticles take longer time to expand. As the intensity of the laser is varied, t_R decreases as the rise in electron temperature is higher. In Fig. 6, we have plotted the absorption coefficient as a function of time for different values of nanoparticle radius. For a given nanoparticle radius, the absorption coefficient rises sharply at $t = t_R$. If the nanoparticle radius is increased the absorption saturates at higher levels.

4. DISCUSSION

The enhancement in laser absorption due to nanostructuring over a metal surface has been observed in many experiments and conjectured that nanostructuring provides stronger laser-material coupling. We believe that the enhancement is caused by the plasmon resonance, that occurs at $\omega_{np0}/\sqrt{3}$ for spherical particles. The absorption is stronger at oblique incidence at all frequencies. The behavior is particularly more explicit for frequencies closer to the resonant frequencies. In cases where differently shaped nanoparticles are present over the surface, the laser resonantly interacts with the particles when $\omega_{np} = \omega\sqrt{\beta}$, where β is an ellipticity

characterizing parameter. For intense short pulses even if this resonance does not occur in the beginning, it can be realized later as the nonlinear heating of nanoparticles and subsequent expansion leads to a reduction in the plasmon requency inside the nanoparticles. For higher laser intensity ($10^{14} W/cm^2$ or higher), the enhancement occurs at an early stage of the pulse because of faster expansion speed owing to the rapid enhancement in electron temperature. These results are in line with the experimental observation of enhancement in laser absorptance due to nanoparticles assisted anomalous absorption. It will be helpful in determining the various parameters for laser assisted ablation experiments also.

REFERENCES

AHMAD, A. & TRIPATHI, V.K. (2006). Nonlinear absorption of a femtosecond laser on a metal surface embedded by metallic nanoparticles. *Appl. Phys. Lett.* **89**, 153112.

AKHMANOV, S.A., EMELYANOV, V.I., KOROTEEV, N.I. & SEMINOGOV, V.N. (1985). Interaction of powerful laser radiation with the surfaces of semiconductors and metals: Nonlinear optical effects and nonlinear optical diagnostics. *Sov. Phys. Usp.* **28**, 1084–1124.

BAGCHI, S., KIRAN, P.P., BHUYAN, M.K., BOSE, S., AYYUB, P., KRISHNAMURTHY, M. & KUMAR, G.R. (2008). Hotter electrons and ions from nano-structured surfaces *Laser Part. Beams* **26**, 259–264.

BIGOT, J.Y., HALTE, V., MERLE, J.C. & DAUNOIS, A. (2000). Electron dynamics in metallic nanoparticles. *Chem. Phys.* **251**, 181–203.

CHEN, Z. & MAO, S. (2008). Femtosecond laser-induced electronic plasma at metal surface. *Appl. Phys. Lett.* **93**, 051506.

DHARESHWAR, L. & CHAURASIA, S. (2008). Laser plasma interaction in solid metal, mixed metal alloy and metal nano-particle coated targets. *J. Phys: Conf. Series* **112**, 032050.

ELIEZER, S., ELIAZ, N., GROSSMAN, E., FISHER, D., GOUZMAN, I., HENIS, Z., PECKER, S., HOROVITZ, Y., FRAENKEL, M., MAMAN, S. & LEREAH, Y. (2004). Synthesis of nanoparticles with femtosecond laser pulses. *Phys. Rev. B* **69**, 144119.

ELIEZER, S., ELIAZ, N., GROSSMAN, E., FISHER, D., GOUZMAN, I., HENIS, Z., PECKER, S., HOROVITZ, Y., FRAENKEL, M., MAMAN, S., EZERSKY, V. & ELIEZER, D. (2005). Nanoparticles and nanotubes induced by femtosecond lasers. *Laser Part. Beams* **23**, 15–19.

ELSAYED-ALI, H.E., NORRIS, T.B., PESSOT, M.A. & MOUROU, G.A. (1987). Time-resolved observation of electron-phonon relaxation in copper. *Phys. Rev. Lett.* **58**, 1212.

FAZIO, E., NERI, F., OSSI, P.M., SANTO, N. & TRUSSO, S. (2009). Ag nanocluster synthesis by laser ablation in Ar atmosphere: A plume dynamics analysis. *Laser Part. Beams* **27**, 281–290.

FUJIMOTO, J.G., LIU, J.M., IPPEN, E.P. & BLOEMBERGEN, N. (1984). Femtosecond laser interaction with metallic tungsten and

nonequilibrium electron and lattice temperatures. *Phys. Rev. Lett.* **53**, 1837–1840.

GAMALY, E.G., RODE, A.V. & LUTHER-DAVIES, B. (2000). Formation of diamond-like carbon films and carbon foam by ultrafast laser ablation. *Laser Part. Beams* **18**, 245–254.

GUREVICH, A.V. (1978). *Nonlinear Phenomena in the Ionosphere.* New York: Springer.

HWANG, T.Y., VOROBYEV, A.Y. & GUO, C. (2009). Ultrafast dynamics of femtosecond laser-induced nanostructure formation on metals. *Appl. Phys. Lett.* **95**, 123111.

JASIAK, R., MANFREDI, G. & HERVIEUX, P.A. (2010). Electron thermalization and quantum decoherence in metal nanostructures. *Phys. Rev. B* **81**, 241401(R).

KAAKKUNEN, J.J.J., PAIVASAARI, K., KUITTINEN, M. & JAASKELAINEN, T. (2009). Morphology studies of the metal surfaces with enhanced absorption fabricated using interferometric femtosecond ablation. *Appl. Phys. A* **94**, 215–220.

KREIBIG, U. & VOLLMER, M. (1995). *Optical Properties of Metal Clusters.* Berlin: Springer.

KUMAR, A. & TRIPATHI, V.K. (2007). Parametric excitation of electron Bernstein waves by radio waves in the ionosphere and its possible consequence for airglow. *J. Phys. D: Appl. Phys.* **40**, 3396–3401.

KUMAR, G. & TRIPATHI, V.K. (2007). Anomalous absorption of surface plasma wave by particles adsorbed on metal surface. *Appl. Phys. Lett.* **93**, 161503.

MAIER, S.A. (2007). *Plasmonics: Fundamentals and Applications.* New York: Springer.

MEISTER, C.-V. & LIPEROVSKY, V.A. (1996). Model of local currents caused by neutral winds in weakly-ionized plasmas. In *Proceeding of the International Conference on the Physics of Strongly Coupled Plasmas.* Singapore: World Scientific, 446–449.

MENENDEZ-MANJON, A., BARCIKOWSKI, S., SHAFEEV, G.A., MAZHUKIN, V.I. & CHICHKOV, B.N. (2010). Influence of beam intensity profile on the aerodynamic particle size distributions generated by femtosecond laser ablation. *Laser Part. Beams* **28**, 45–52.

NOLTE, S., CHICHKOV, B.N., WELLING, H., SHANI, Y., LIEBERMANN, K. & TERKEL, H. (1999). Nanostructuring with spatially localized femtosecond laser pulses. *Opt. Lett.* **24**, 914.

PUSTOVALOV, V.K. (2005). Theoretical study of heating of spherical nanoparticle in media by short laser pulses. *Chem. Phys.* **308**, 103–108.

RAJEEV, P.P., TANEJA, P., AYYUB, P., SANDHU, A.S. & KUMAR, G.R. (2003). Metal Nanoplasmas as Bright Sources of Hard X-Ray Pulses. *Phys. Rev. Lett.* **90**, 115002.

SHUKLA, G. & KHARE, A. (2010). Spectroscopic studies of laser ablated ZnO plasma and correlation with pulsed laser deposited ZnO thin film properties. *Laser Part. Beams* **28**, 149–55.

STRATAKIS, E., ZORBA, V., BARBEROGLOU, M., FOTAKIS, C. & SHAFEEV, G.A. (2009). Generation of nanostructures on metals by laser ablation in liquids: New results. *Nanotechnol.* **20**, 105303.

TAYLOR, D.P. & HELVAJIAN, H. (2009). Volume plasmon ejection of ions in pulsed ultraviolet laser induced desorption from several metals. *Phys. Rev. B* **79**, 075411.

THAREJA, R.K. & SHARMA, A.K. (2006). Reactive pulsed laser ablation: Plasma studies. *Laser Part. Beams* **24**, 311–320.

VOROBYEV, A.Y. & GUO, C. (2005a). Direct observation of enhanced residual thermal energy coupling to solids in femtosecond laser ablation. *Appl. Phys. Lett.* **86**, 011916.

VOROBYEV, A.Y. & GUO, C. (2005b). Enhanced absorptance of gold following multipulse femtosecond laser ablation. *Phys. Rev. B* **72**, 195422.

VOROBYEV, A.Y. & GUO, C. (2006). Enhanced energy coupling in femtosecond laser-metal interactions at high intensities. *Opt. Express* **14**, 13113.

VOROBYEV, A.Y. & GUO, C. (2008). Colorizing metals with femtosecond laser pulses. *Appl. Phys. Lett.* **92**, 041914.

VOROBYEV, A.Y., MAKIN, V.S. & GUO, C. (2009). Brighter light sources from black metal: Significant increase in emission efficiency of incandescent light sources. *Phys. Rev. Lett.* **102**, 234301.

WIEGER, V., STRASSL, M. & WINTNER, E. (2006). Pico- and microsecond laser ablation of dental restorative materials. *Laser Part. Beams* **24**, 41–45.

WOLOWSKY, J., BADZIAK, J., CZARNECKA, A., PARYS, P., PISAREK, P., ROSINSKI, M., TURAN, R. & YERCI, S. (2007). Application of pulsed laser deposition and laser-induced ion implantation for formation of semiconductor nano-crystallites. *Laser Part. Beams* **25**, 65–69.

ZAVESTOVSKAYA, I.N. (2010). Laser-assisted metal surface micro- and nanostructurization. *Laser Part. Beams* **28**, 437–442.